Available online at www.sciencedirect.com
ScienceDirect
Journal of the European Ceramic Society 30 (2010) 2585–2592
www.elsevier.com/locate/jeurceramsoc

Microwave dielectric properties of novel temperature stable high Q $Li_2Mg_{1-x}Zn_xTi_3O_8$ and $Li_2A_{1-x}Ca_xTi_3O_8$ (A = Mg, Zn) ceramics

Sumesh George, Mailadil Thomas Sebastian *

Materials and Minerals Division, National Institute for Interdisciplinary Science and Technology, Thiruvananthapuram 695019, India

Received 19 January 2010; received in revised form 4 May 2010; accepted 16 May 2010
Available online 11 June 2010

Abstract

The $Li_2Mg_{1-x}Zn_xTi_3O_8$ ($x = 0$–1) and $Li_2A_{1-x}Ca_xTi_3O_8$ (A = Mg, Zn and $x = 0$–0.2) ceramics are synthesized by solid-state ceramic route and the microwave dielectric properties are investigated. The $Li_2MgTi_3O_8$ ceramic shows $\varepsilon_r = 27.2$, $Q_u \times f = 42{,}000$ GHz, and $\tau_f = (+)3.2$ ppm/°C and $Li_2ZnTi_3O_8$ has $\varepsilon_r = 25.6$, $Q_u \times f = 72{,}000$ GHz, and $\tau_f = (-)11.2$ ppm/°C respectively when sintered at 1075 °C/4 h. The $Li_2Mg_{0.9}Zn_{0.1}Ti_3O_8$ dielectric ceramic composition shows the best dielectric properties with $\varepsilon_r = 27$, $Q_u \times f = 62{,}000$ GHz, and $\tau_f = (+)1.1$ ppm/°C. The effect of Ca substitution on the structure, microstructure and microwave dielectric properties of $Li_2A_{1-x}Ca_xTi_3O_8$ (A = Mg, Zn and $x = 0$–0.2) has also been investigated. The materials reported in this paper are excellent in terms of dielectric properties and cost of production compared to commercially available high Q dielectric resonators.

Keywords: Microwave dielectrics; Resonator; LMT; LZT

1. Introduction

In pace with the advances in microwave telecommunication and satellite broadcasting, a variety of microwave devices have been developed using dielectric resonators and the resonators have become indispensable components in microwave communication systems.[1–4] The microwave dielectric materials are advantageous in terms of compactness, light weight, temperature stability and low cost in the production of high frequency devices.[5,6] The current trend and the state of the art of microwave dielectric materials for telecommunication applications are discussed in a recent book "Dielectric materials for wireless communications".[4] The complex perovskites such as $Ba(Zn_{1/3}Ta_{2/3})O_3$ (BZT) and $Ba(Mg_{1/3}Ta_{2/3})O_3$ (BMT) show the highest quality factor ($Q \times f > 150{,}000$) with low τ_f.[7–9] However, they are made up of expensive chemicals such as tantalates or niobates. The $(Zr_{1-x}Sn_x)TiO_4$, $Ba_2Ti_9O_{20}$, $BaTi_4O_9$ are some low cost materials which show useful microwave dielectric properties.[10–12] However, high sintering temperature together with a long annealing time is necessary for obtaining excellent microwave dielectric properties. Hence, these high Q dielectric ceramics are not cost effective either in terms of its cost of raw materials or its high processing temperature. A variety of microwave devices have been developed using dielectric resonators as the frequency determining components. However, due to the constraints of size, frequency of operation, frequency stability and selectivity, only those materials with high relative permittivity (ε_r), low dielectric loss and nearly zero temperature coefficient of resonant frequency (τ_f) can meet the requirements for DR applications.[1,3,4,13,14] Another constraint in making light weight electronic modules is the high density (≈ 5 g/cm^3) of dielectric ceramics and the cost of production. These requirements put constraints on the number of materials available for DR applications. The reported dielectric materials in the literature so far have failed either atleast one of its important properties such as cost of the raw materials, sintering temperature, permittivity, quality factor, temperature coefficient of resonant frequency, or bulk density. Achieving all these requirements in one material is a formidable task and optimal balance of these properties is one of the major challenges in the electronic industry. Recently West et al. reported the crystal structure of ternary spinal such as $Li_2MgTi_3O_8$ and $Li_2ZnTi_3O_8$ ceramics.[15,16] However, their electrical properties have not been reported so far.

* Corresponding author. Tel.: +91 471 2515294; fax: +91 471 2491712.
E-mail address: mailadils@yahoo.com (M.T. Sebastian).

0955-2219/$ – see front matter © 2010 Elsevier Ltd. All rights reserved.
doi:10.1016/j.jeurceramsoc.2010.05.010

This paper discusses the synthesis, characterization and microwave dielectric properties of novel low loss dielectric materials ($Li_2Mg_{1-x}Zn_xTi_3O_8$ ($x = 0$–1) and $Li_2A_{1-x}Ca_xTi_3O_8$ (A = Mg, Zn and $x = 0$–0.2)) having spinel structure which satisfies all the above mentioned requirements and can address the growing demand of microelectronic industry.

2. Experimental

The $Li_2Mg_{1-x}Zn_xTi_3O_8$ ($x = 0$–1) and $Li_2A_{1-x}Ca_xTi_3O_8$ (A = Mg, Zn and $x = 0$–0.2) ceramic samples were prepared by the conventional solid-state ceramic route. High purity Li_2CO_3, ZnO, $(MgCO_3)_4$ $Mg(OH)_2$ $5H_2O$, $CaCO_3$ and TiO_2 (99.9+%, Aldrich Chemical Company, Inc., Milwaukee, WI, USA) were used as the starting materials. Stoichiometric amounts of the powder samples were mixed and ball milled using zirconia balls in ethanol medium for 24 h. The resultant slurry was then dried and calcined at 900 °C/4 h. The calcined powders were ground to form fine powders and polyvinyl alcohol (PVA) (molecular weight 72,000, BDH Lab Suppliers, England) solution was then added to the powder, mixed, dried and ground well and pressed into cylindrical disks of about 14 mm diameter and 7 mm thickness, by applying a pressure of about 100 MPa. These compacts were muffled by powder of the same composition and sintered at different temperatures in the range 1000–1125 °C/4 h. The sintering temperature was optimized for the best density and dielectric properties. The crystal structure and phase purity of the powdered samples were studied by X- ray diffraction technique using Ni-filtered Cu-Kα radiation using Rigaku Dmax-I, Japan, diffractometer. The microstructures of the sintered samples were studied using scanning electron microscope (JEOL-JSM 5600 LV, Tokyo, Japan). The sintered density of the specimen was measured by the Archimedes method. The microwave dielectric properties were measured in the frequency range 4–6 GHz by a Vector Network Analyzer (8753 ET, Agilent Technologies). The dielectric constant and unloaded quality factor of the samples were measured by Hakki and Coleman and cavity methods respectively.[4,17,18]

3. Results and discussion

3.1. Phase analysis and the microwave dielectric properties of $Li_2Mg_{1-x}Zn_xTi_3O_8$ ceramics

Fig. 1 shows the variation of the relative density of $Li_2MgTi_3O_8$ (LMT) and $Li_2ZnTi_3O_8$ (LZT) ceramics calcined at 900 °C/4 h as a function of sintering temperature. As the sintering temperature increased to 1075 °C/4 h, the relative density increased to a maximum value and further increase in sintering temperature decreased the density. The improvement in densification could be due to the elimination of pores in the ceramics. A maximum densification of 95.5% and 95% is observed for LMT and LZT ceramics respectively at a sintering temperature of 1075 °C/4 h. It is reported that lithium is volatile and escapes at high sintering temperatures.[19,20] The decreased densification at higher sintering temperature could be due to the trapped porosity by the evaporation of lithium and also due to the abnormal grain growth.

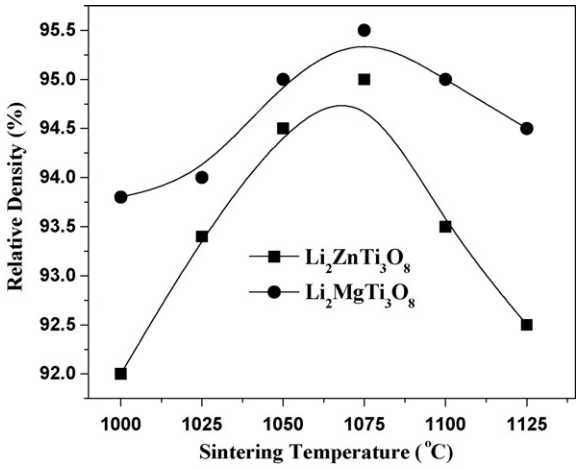

Fig. 1. Variation of relative density of (a) $Li_2MgTi_3O_8$ and (b) $Li_2ZnTi_3O_8$ ceramics as a function of sintering temperature.

Fig. 2 shows the X-ray diffraction pattern of $Li_2Mg_{1-x}Zn_xTi_3O_8$ ($x = 0$, 0.1, 0.2, 0.3, 0.4, 0.6, 0.8, and 1) ceramics sintered at its optimized sintering temperature of 1075 °C/4 h. All the peaks are indexed based on JCPDS file number 48-0263 for $Li_2MgTi_3O_8$ and 86-1512 for $Li_2ZnTi_3O_8$ with cubic crystal symmetry. The strongest peak is observed at $2\theta = 18.2995$ ($d = 4.8442$) for $Li_2MgTi_3O_8$ and $2\theta = 35.526$ ($d = 2.52488$) for $Li_2ZnTi_3O_8$ respectively. As x increases in $Li_2Mg_{1-x}Zn_xTi_3O_8$ ceramics, a sudden shift of strongest intensity peak from $2\theta = 18.2995$ to 35.526 is observed. This shift is observed near $x = 0.1$. As x increases, the cell parameter and the cell volume of $Li_2Mg_{1-x}Zn_xTi_3O_8$ decrease as shown in Fig. 3. The lattice parameter is $a = 8.381(4)$ Å for $Li_2MgTi_3O_8$ and $a = 8.372(2)$ Å for $Li_2ZnTi_3O_8$ which is consistent with corresponding reported JCPDS files. The $Li_2Mg_{1-x}Zn_xTi_3O_8$ ceramic has a cubic symmetry and the lattice parameter is calculated by plotting 'a' versus $\sin^2(\theta)$.[21] A straight line

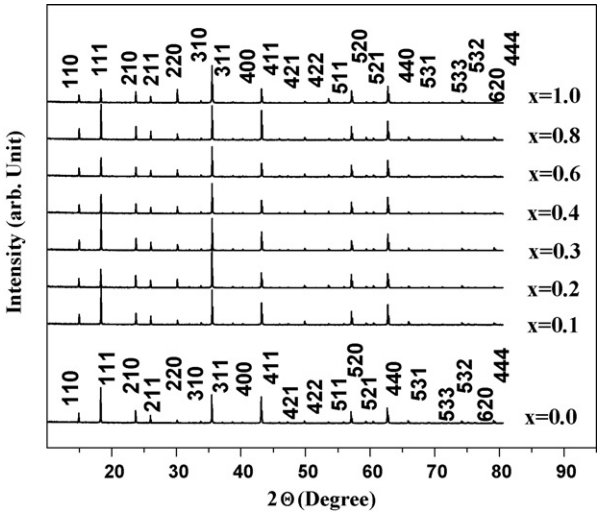

Fig. 2. X-ray diffraction patterns of $Li_2Mg_{1-x}Zn_xTi_3O_8$ ($x = 0$, 0.1, 0.2, 0.3, 0.4, 0.6, 0.8, and 1) ceramics sintered at 1075 °C/4 h.

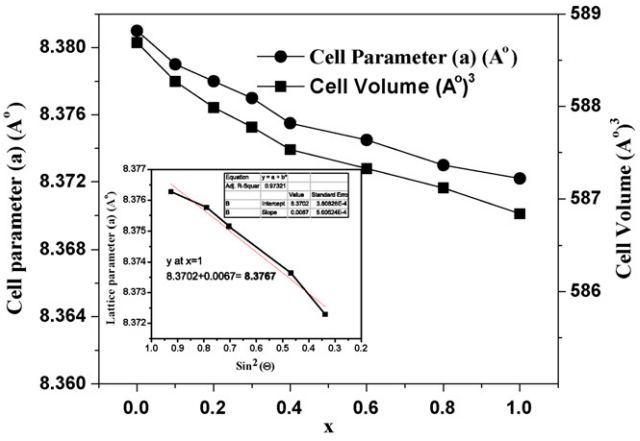

Fig. 3. The variation of lattice parameter and the cell volume of $Li_2Mg_{1-x}Zn_xTi_3O_8$ ($x = 0$, 0.1, 0.2, 0.3, 0.4, 0.6, 0.8, and 1) ceramics sintered at 1075 °C/4 h as a function of x. Inset shows the extrapolation of the lattice parameter.

is formed and extrapolation of this line to $\sin^2(\theta) = 1$ gives the value of lattice parameter 'a'. Inset of Fig. 3 shows the extrapolation of the lattice parameter 'a' for the composition $Li_2Mg_{0.9}Zn_{0.1}Ti_3O_8$ ceramics.

Fig. 4 shows the SEM images of thermally etched (25 °C below the optimized sintering temperature) (a) $Li_2MgTi_3O_8$ and (b) $Li_2ZnTi_3O_8$ ceramics sintered at 1075 °C/4 h. The grains are closely packed and a small amount of porosity can be observed. The majority of the grains are having an average size of 30–40 μm. However, smaller grains are also observed for both the compositions. Fig. 4 also shows the SEM micrograph of the thermally etched $Li_2Mg_{1-x}Zn_xTi_3O_8$ (c) $x = 0.2$, (d) $x = 0.4$ (e) $x = 0.6$ and (f) $x = 0.8$. All the SEM images except Fig. 4(c) ($x = 0.2$) show similar microstructure and Fig. 4(c) shows a porous microstructure. Two types of grains having different contrast are observed in Fig. 4(e). Fig. 4(g) is the magnified image of Fig. 4(e) which confirms the phase purity.

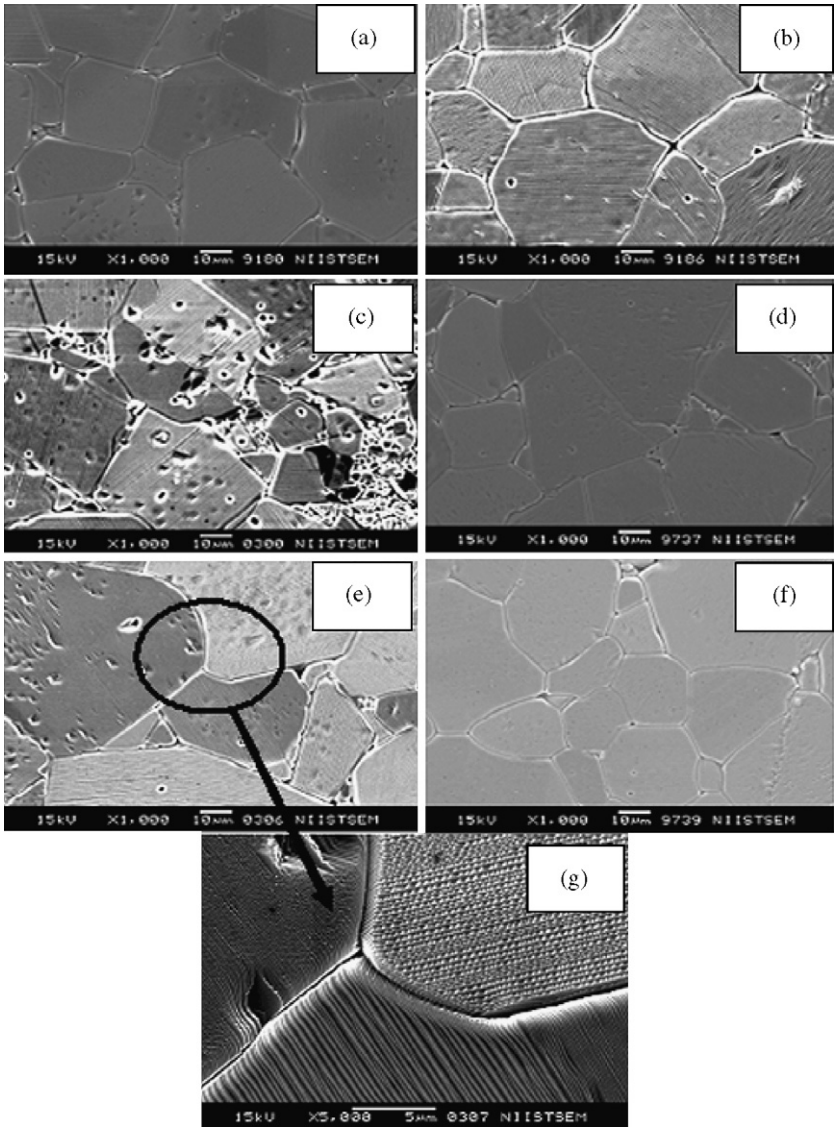

Fig. 4. SEM images of thermally etched $Li_2Mg_{1-x}Zn_xTi_3O_8$ ceramics (a) $x = 0$, (b) $x = 1$, (c) $x = 0.2$, (d) $x = 0.4$, (e) $x = 0.6$, (f) $x = 0.8$, and (g) magnified image of $x = 0.6$.

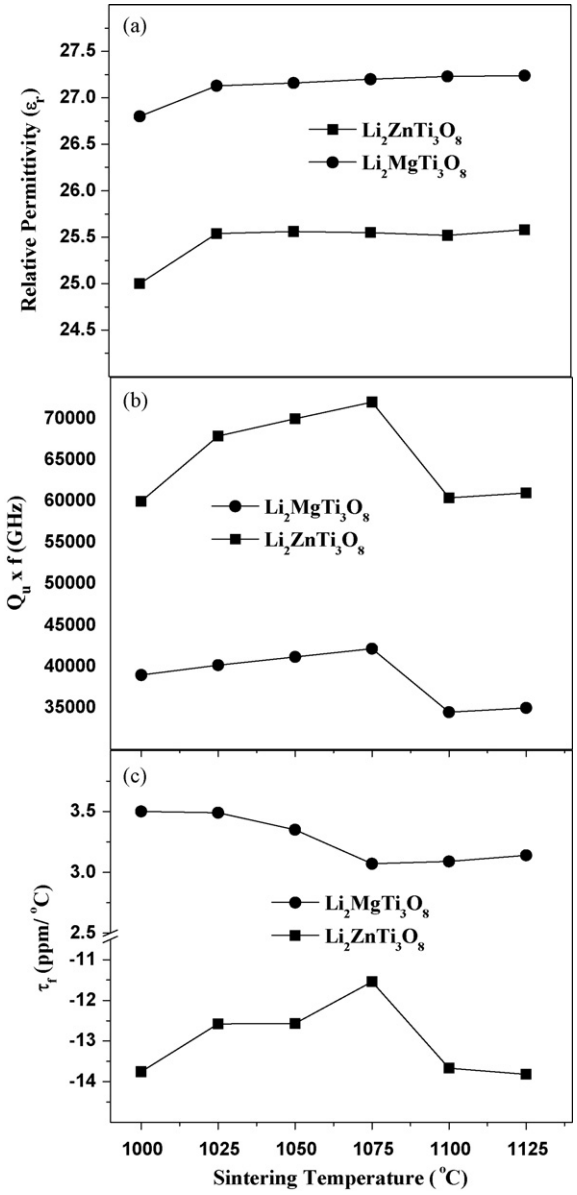

Fig. 5. The variation of (a) relative permittivity, (b) quality factor and (c) temperature coefficient of resonant frequency $Li_2MgTi_3O_8$ and $Li_2ZnTi_3O_8$ ceramics as a function of sintering temperature.

Fig. 5 shows the variation of (a) relative permittivity (b) quality factor and (c) temperature coefficient of resonant frequency of $Li_2MgTi_3O_8$ (LMT) and $Li_2ZnTi_3O_8$ (LZT) ceramics as a function of sintering temperature. It can be observed that the variation of microwave dielectric properties of LMT and LZT ceramics with sintering temperature is similar to that of densification. The best dielectric properties are observed for the best densification. As the sintering temperature increases to 1075 °C/4 h, the relative permittivity and quality factor reached maximum values and the temperature coefficient of resonant frequency is found to be minimum. However, subsequent increase in sintering temperature degrades the microwave dielectric properties. The improvements in microwave dielectric properties are attributed to the densification. On the other hand, the dielectric properties are degraded due to the poor densification by the escape of volatile element such as lithium at elevated temperatures.[19,20] The $Li_2MgTi_3O_8$ ceramics sintered at 1075 °C/4 h has $\varepsilon_r = 27.2$ and $Q_u \times f = 42{,}000$ GHz and $\tau_f = (+)3.2$ ppm/°C at 5 GHz. The $Li_2ZnTi_3O_8$ ceramics sintered at 1075 °C/4 h shows $\varepsilon_r = 25.6$ and $Q_u \times f = 72{,}000$ GHz and $\tau_f = (-)11.2$ ppm/°C at 5 GHz. It has been observed that the $Li_2MgTi_3O_8$ and $Li_2ZnTi_3O_8$ ceramics show excellent microwave dielectric properties and hence the $Li_2Mg_{1-x}Zn_xTi_3O_8$ solid solutions have been prepared with a view of tailoring the dielectric properties.

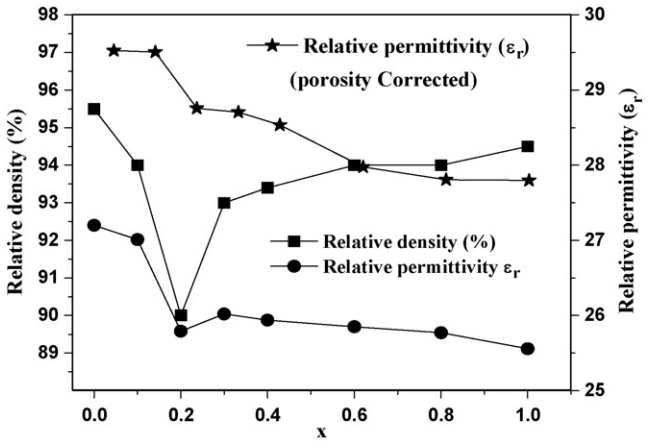

Fig. 6. The variation of densification and the relative permittivity of $Li_2Mg_{1-x}Zn_xTi_3O_8$ ceramic as a function of x.

Fig. 6 shows the densification and the relative permittivity of $Li_2Mg_{1-x}Zn_xTi_3O_8$ ceramic as a function of x. The densification of $Li_2Mg_{1-x}Zn_xTi_3O_8$ ceramics is expected to be in between the densities of the end compositions. However, a sharp decrease in densification (90% of theoretical density) is observed in the vicinity of $x = 0.2$. This composition is very difficult to sinter and increasing the sintering temperature further decreased the density of the samples. The SEM picture (see Fig. 4(c); $x = 0.2$) indicates poor densification of this composition. Fig. 6 shows the variation of relative permittivity of $Li_2Mg_{1-x}Zn_xTi_3O_8$ ceramics as a function of x. When x increased from 0 to 1, the relative permittivity of $Li_2Mg_{1-x}Zn_xTi_3O_8$ ceramics decreased from 27.2 to 25.6. All the compositions of $Li_2Mg_{1-x}Zn_xTi_3O_8$ ceramics show a densification of about 93–95.5%. The porosity corrected permittivity of $Li_2Mg_{1-x}Zn_xTi_3O_8$ ceramics is calculated using the equation[4,22]:

$$\varepsilon_r = \varepsilon_r' \left(1 - \frac{3P\left(\varepsilon_r' - 1\right)}{2\varepsilon_r' + 1}\right)$$

where ε_r' is the permittivity of the material corrected for porosity, ε_r is the experimentally obtained permittivity and P is the fractional porosity.

The porosity corrected relative permittivity of $Li_2Mg_{1-x}Zn_xTi_3O_8$ ceramics shows a decrease with an increase in x. As x increased from 0 to 1, the porosity corrected relative permittivity of $Li_2Mg_{1-x}Zn_xTi_3O_8$ ceramics decreased from 29.5 to 27.8.

Fig. 7 shows the variation of quality factor and the temperature coefficient of resonant frequency (τ_f) of

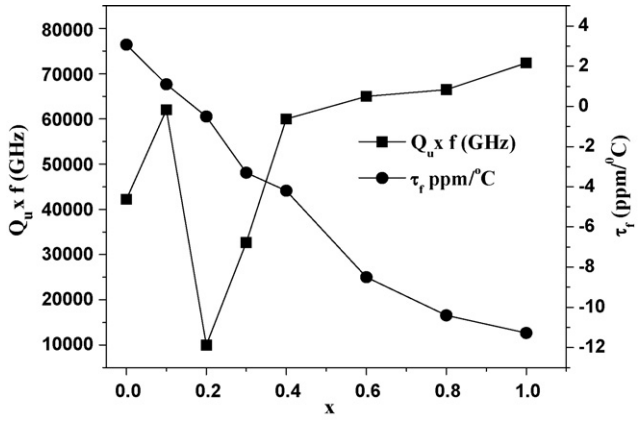

Fig. 7. The variation of quality factor and the temperature coefficient of resonant frequency of $Li_2Mg_{1-x}Zn_xTi_3O_8$ ceramics sintered at 1075 °C/4 h as a function of x.

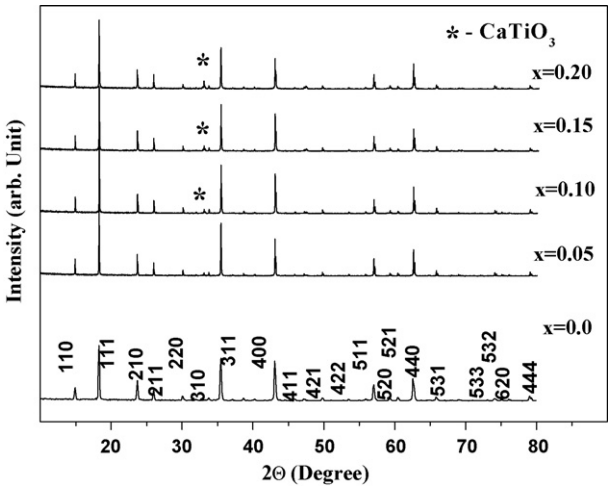

Fig. 8. X-ray diffraction patterns of $Li_2Mg_{1-x}Ca_xTi_3O_8$ ($x = 0$, 0.05, 0.10, 0.15, and 0.20) ceramics sintered at 1075 °C/4 h.

$Li_2Mg_{1-x}Zn_xTi_3O_8$ ceramics sintered at 1075 °C/4 h as a function of x. The quality factor of $Li_2MgTi_3O_8$ and $Li_2ZnTi_3O_8$ ceramics are 42,000 and 72,000 GHz respectively. Hence the quality factor of $Li_2Mg_{1-x}Zn_xTi_3O_8$ ceramics sintered at 1075 °C/4 h is expected to be in between the quality factors of the end compositions. As x increases from 0 to 0.1, the quality factor of $Li_2Mg_{1-x}Zn_xTi_3O_8$ ceramics increases from 42,000 to 62,000 GHz. However, subsequent increase in x ($x = 0.2$), the $Li_2Mg_{1-x}Zn_xTi_3O_8$ ceramics show poor resonance ($Q_u \times f$ of about 10,000 GHz). The extrinsic factors such as poor densification and the associated trapped porosity may be the reason for the low quality factor for $x = 0.2$. However, from Fig. 7 it can be observed that further increase in x value increases the quality factor of $Li_2Mg_{1-x}Zn_xTi_3O_8$ ceramics. The variation of temperature coefficient of resonant frequency of $Li_2Mg_{1-x}Zn_xTi_3O_8$ ceramics sintered at 1075 °C/4 h as a function of x is also shown in Fig. 7. It is noted that, as x increases from 0 to 1, the τ_f of $Li_2Mg_{1-x}Zn_xTi_3O_8$ ceramics varies from (+)3.1 to (−)11.2 ppm/°C.

The well-known microwave dielectric materials with high quality factor in general need high sintering temperature together with long soaking time.[4] However, the $Li_2MgTi_3O_8$ and $Li_2ZnTi_3O_8$ dielectric ceramics in the present investigation show excellent dielectric properties at a relatively low sintering temperature of 1075 °C/4 h. The microwave dielectric losses in bulk ceramics fall into two categories, intrinsic and extrinsic.[23,24] In a recent study on clean grain boundaries in MgO crystals, Alford et al.[25] concluded that at room temperature grain boundaries have a limited influence on MW dielectric loss. However, in sintered alumina, dielectric loss is found to depend strongly on pore size, pore volume, and grain size.[22] The interplay of parameters such as porosity, liquid phase and cation ordering makes it difficult for researchers to make definitive remark on the relationship between grain size and dielectric loss in the polycrystalline microwave dielectric ceramics. Report shows that impurities even in minor amount will cause an increase in the dielectric loss of ceramics.[26] The sintering process sweeps impurities to the grain boundaries and hence the impurities and grain boundaries are inextricably linked.[25] For small grains, there is a possibility of accumulation of impurities at the grain boundaries which is less for larger grains and this markedly affects the quality factor. Hence, it is reasonable to assume that if grain boundaries are a source of dielectric loss, then reducing their number might be expected to reduce the dielectric loss.[22] It is generally accepted that ceramics having larger grains shows relatively better microwave dielectric properties in addition to the inherent properties. From the SEM image it is worth to note that both the ceramics are having the grain size of about 30–40 μm. The large grain size of the $Li_2MgTi_3O_8$ and $Li_2ZnTi_3O_8$ ceramics could be reason for the high quality factor when sintered at 1075 °C/4 h.

3.2. Effect of Ca substitution on the microwave dielectric properties of $Li_2(A_{1-x}Ca_x)Ti_3O_8$ ceramics (A = Mg, Zn)

It has been reported that substitution always alters the dielectric properties depending on the chemical reactivity, solid solubility and the formation of the second phase of substituting element with the parent composition.[27] In the previous section we have seen that zinc acts as good substitutant for magnesium in the composition $Li_2(Mg_{1-x}Zn_x)Ti_3O_8$ and improved the quality factor. The ionic radii of zinc (0.74 Å) and magnesium (0.72 Å) are comparable. Calcium has a slightly higher ionic radii (1.0 Å) as compared to zinc and magnesium (CN = 6). The present section discusses the effect of substitution of elements having higher ionic radius (calcium) on the microwave dielectric properties of $Li_2(A_{1-x}Ca_x)Ti_3O_8$ ceramics (A = Mg, Zn and $x = 0$, 0.05, 0.1, 0.15, and 0.20) ceramics.

Figs. 8 and 9 show the X-ray diffraction pattern of $Li_2(A_{1-x}Ca_x)Ti_3O_8$ ceramics (A = Mg, Zn and $x = 0$, 0.05, 0.1, 0.15, and 0.20) ceramics sintered at 1075 °C/4 h. All the peaks in Fig. 8 are indexed based on JCPDS file number 48-0263 for Ca substituted $Li_2MgTi_3O_8$ ceramics and Fig. 9 is indexed based on JCPDS file number 86-1512 for Ca substituted $Li_2ZnTi_3O_8$ ceramics with cubic crystal symmetry. A small amount of second phase ($CaTiO_3$) has been observed for the calcium substituted $Li_2(A_{1-x}Ca_x)Ti_3O_8$ ceramics (A = Mg, Zn and $x = 0$, 0.05, 0.1,

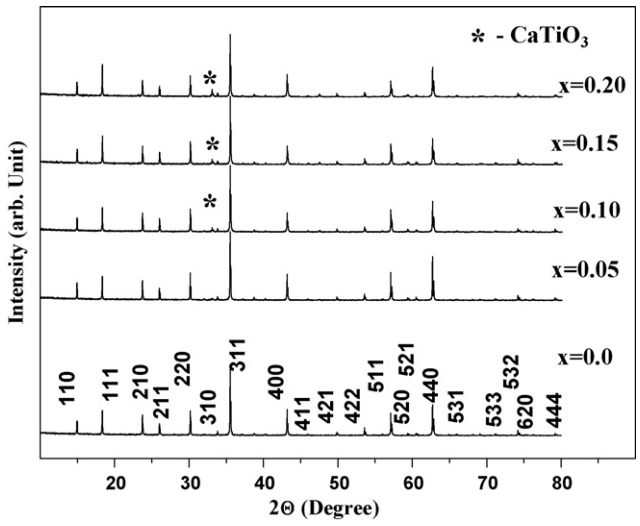

Fig. 9. X-ray diffraction patterns of $Li_2Zn_{1-x}Ca_xTi_3O_8$ ($x = 0$, 0.05, 0.10, 0.15, and 0.20) ceramics sintered at 1075 °C/4 h.

0.15, and 0.20) ceramics. The intensity of second phase is found to increase with increase in the calcium substitution. The formation of the second phase could be due to the difficulty in fully substituting the relatively large calcium ions as compared to that of magnesium and zinc. The second phase observed is $CaTiO_3$ and is indexed based on the JCPDS file 42-0423. In the case of Ca substitution for Mg, second phase is formed for $x = 0.05$ and the $CaTiO_3$ content increases with increase in x value. The intensity of XRD peaks corresponding to $CaTiO_3$ increase with Ca substitution. In the case of Zn, the $CaTiO_3$ XRD peaks start appearing at $x = 0.1$ and the intensity of XRD peaks corresponding to $CaTiO_3$ increase with increase in x.

Fig. 10 shows the microstructure of $Li_2(A_{1-x}Ca_x)Ti_3O_8$ (A = Mg, Zn) ceramics for different Ca content. The grains have an average size of about 30–40 μm. By comparing Figs. 4 and 10, it can be observed that the substitution of calcium does not change much the grain morphology or grain size. However, small amount of second phase ($CaTiO_3$) which is randomly distributed on the grains and grain boundaries is observed. The mixture phase observed in the microstructure support the secondary phase detected in the X-ray diffraction patterns of $Li_2(A_{1-x}Ca_x)Ti_3O_8$ (A = Mg, Zn) ceramics. The $CaTiO_3$ second phase is marked in the inset of Fig. 10(b).

Fig. 11(a) shows the variation of density of $Li_2(A_{1-x}Ca_x)Ti_3O_8$ (A = Mg, Zn) ceramics as a function of x. It is clear from the SEM images that increase in the Ca substitution increases porosity. Hence it is expected to decrease the density of the $Li_2(Mg_{1-x}Ca_x)Ti_3O_8$ ceramics with Ca substitution. A slight decrease in density is observed for the Ca substitution (up to $x = 0.05$) for $Li_2(Mg_{1-x}Ca_x)Ti_3O_8$ ceramics. However, further increase in Ca substitution increases the density slightly. The second phase ($CaTiO_3$) has slightly higher density (4.036 g/cm^3) compared to that of LMT and LZT ceramics.[4,28,29] The increase in the density of $Li_2(Mg_{1-x}Ca_x)Ti_3O_8$ with an increase in Ca substitution could be due to the increased amount of $CaTiO_3$ second phase. The slight decrease in density of $Li_2(Zn_{1-x}Ca_x)Ti_3O_8$ with an increase in Ca substitution could be due to the formation of pores and which seems to be more for $Li_2(Zn_{1-x}Ca_x)Ti_3O_8$ compared to $Li_2(Mg_{1-x}Ca_x)Ti_3O_8$ (see Fig. 10). As the Ca substitution increases from 0 to 0.20, the density of $Li_2(Mg_{1-x}Ca_x)Ti_3O_8$ increases from 3.31 to 3.41 g/cm^3 and that of $Li_2(Zn_{1-x}Ca_x)Ti_3O_8$ varies from 3.77 to 3.74 g/cm^3. Fig. 11(b) shows the variation of relative permittivity of $Li_2(A_{1-x}Ca_x)Ti_3O_8$ (A = Mg, Zn) ceramics as a function of calcium substitution. The relative permittivity is found to increase with an increase in the calcium substitution for both the $Li_2(Mg_{1-x}Ca_x)Ti_3O_8$ and $Li_2(Zn_{1-x}Ca_x)Ti_3O_8$ ceramics. The

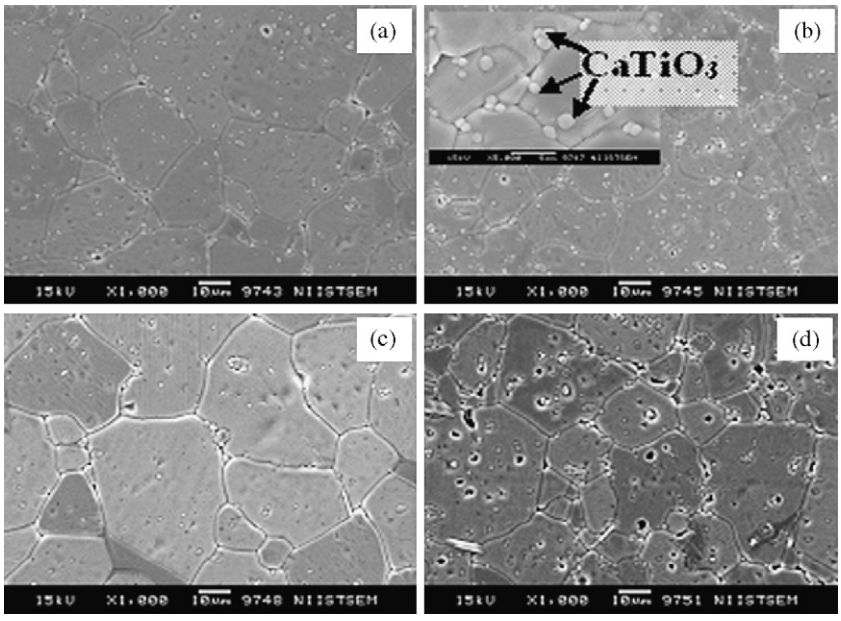

Fig. 10. SEM images of $Li_2(A_{1-x}Ca_x)Ti_3O_8$ (a) A = Mg and $x = 0.10$, (b) A = Mg and $x = 0.20$, (c) A = Zn and $x = 0.10$, and (d) A = Zn and $x = 0.20$ ceramics sintered at 1075 °C/4 h.

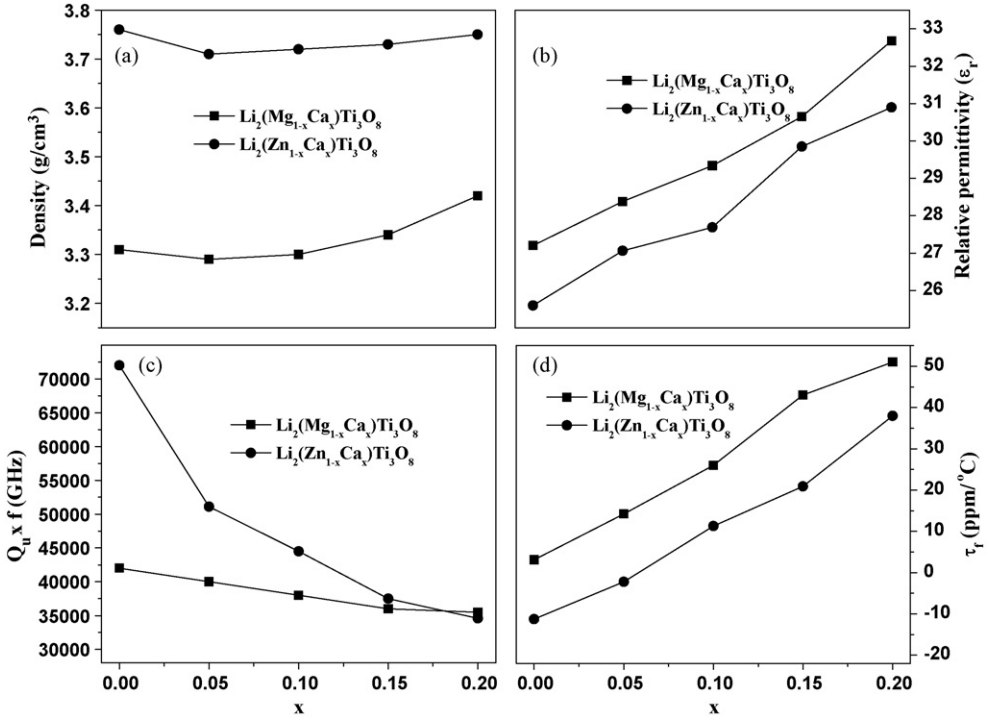

Fig. 11. Variation of (a) density, (b) relative permittivity, (c) quality factor, and (d) temperature coefficient of resonant frequency of $Li_2(A_{1-x}Ca_x)Ti_3O_8$ (A = Mg, Zn) ceramics as a function of x.

$CaTiO_3$ has a permittivity of about 174[4,28,29] which is much higher than that of $Li_2MgTi_3O_8$ and $Li_2ZnTi_3O_8$ ceramics. The higher permittivity of the second phase could be the reason for the increase in the permittivity of $Li_2(A_{1-x}Ca_x)Ti_3O_8$ (A = Mg, Zn) ceramics with calcium content. As x increases from 0 to 0.2, the relative permittivity of $Li_2(Mg_{1-x}Ca_x)Ti_3O_8$ and $Li_2(Zn_{1-x}Ca_x)Ti_3O_8$ ceramics increases from 27.2 to 32.7 and 25.6 to 30.9 respectively. The variation of quality factor of $Li_2(A_{1-x}Ca_x)Ti_3O_8$ (A = Mg, Zn) ceramics as a function of calcium content is shown in Fig. 11(c). The quality factor of both $Li_2(Mg_{1-x}Ca_x)Ti_3O_8$ and $Li_2(Zn_{1-x}Ca_x)Ti_3O_8$ ceramics is found to decrease with increase in the calcium substitution. The $CaTiO_3$ has a low quality factor of about 3600 GHz[4,28,29] compared to $Li_2MgTi_3O_8$ and $Li_2ZnTi_3O_8$ ceramics. Hence the $CaTiO_3$ phase having lower quality factor could be the reason for the decrease in the quality factor of $Li_2(A_{1-x}Ca_x)Ti_3O_8$ (A = Mg, Zn) ceramics. Fig. 11(d) depicts the variation of the temperature coefficient of resonant frequency of $Li_2(A_{1-x}Ca_x)Ti_3O_8$ (A = Mg, Zn) ceramics as a function of calcium substitution. The τ_f of $Li_2(Mg_{1-x}Ca_x)Ti_3O_8$ increases from (+)3.1 to (+)51 ppm/°C where as the τ_f of $Li_2(Zn_{1-x}Ca_x)Ti_3O_8$ shifts from −11.21 to +38 ppm/°C. It is well known that the $CaTiO_3$ has a high positive τ_f of about (+800 ppm/°C) and it is commonly used to tune the temperature coefficient of resonant frequency of microwave dielectric ceramics which are having a negative τ_f[30,31] The high positive τ_f of the $CaTiO_3$ second phase could be the reason for the increase in the τ_f of $Li_2(A_{1-x}Ca_x)Ti_3O_8$ (A = Mg, Zn) ceramics with calcium content.

4. Conclusions

The $Li_2Mg_{1-x}Zn_xTi_3O_8$ (x = 0–1) and $Li_2A_{1-x}Ca_xTi_3O_8$ (A = Mg, Zn and x = 0–0.2) ceramic samples are prepared by the conventional solid-state ceramic route and the phase purity, microstructure and microwave dielectric properties are investigated. The $Li_2MgTi_3O_8$ and $Li_2ZnTi_3O_8$ ceramics shows $\varepsilon_r = 27.2$, $Q_u \times f = 42{,}000$ GHz, and $\tau_f = (+)3.2$ and $\varepsilon_r = 25.6$, $Q_u \times f = 72{,}000$ GHz, and $\tau_f = (-)11.2$ ppm/°C respectively when sintered at 1075 °C/4 h. Among all the compositions of $Li_2Mg_{1-x}Zn_xTi_3O_8$ ceramics, the $Li_2Mg_{0.9}Zn_{0.1}Ti_3O_8$ dielectric ceramic composition shows the best dielectric properties such as $\varepsilon_r = 27$, $Q_u \times f = 62{,}000$ GHz, and $\tau_f = (+)1.1$ ppm/°C when sintered at 1075 °C/4 h. The effect of Ca substitution on the structure and microwave dielectric properties of $Li_2A_{1-x}Ca_xTi_3O_8$ (A = Mg, Zn and x = 0–0.2) has been investigated and it is found that formation of second phase degrades the microwave dielectric properties slightly. The $Li_2(Mg_{1-x}Zn_x)Ti_3O_8$ ceramics developed in the present investigation has excellent microwave dielectric properties compared to commercially available dielectric resonators. The low sintering temperature with inexpensive raw materials makes the new composition very attractive.

Acknowledgements

The authors are grateful to the CSIR and DST, New Delhi, for the financial assistance.

References

1. Makimoto M, Yamashita S. *Microwave resonators and filters for wireless communication: theory, design and application*. Berlin, Heidelberg: Springer; 2001.
2. Wakino K, Nishikawa T, Tamura S, Ishikawa Y. Microwave bandpass filters containing dielectric resonator with improved temperature stability and spurious response. *IEEE MTT-S Int Microwave Symp Dig* 1975.
3. Wersing W. Microwave ceramics for resonators and filters. *Curr Opin Solid State Mater Sci* 1996;**1**:715–31.
4. Sebastian MT. *Dielectric materials for wireless communications*. Oxford, UK: Elsevier Publishers; 2008.
5. Freer R. Microwave dielectric ceramics—an overview. *Silic Indus* 1993;**9–10**:191–7.
6. Sethares JC, Naumann SJ. Design of microwave dielectric resonators. *Trans Microwave Theory Technol* 1966;**MTT-14**:2–7.
7. Kawashima S, Nishida M, Ueda I, Ouchi H. $Ba(Zn,Ta)O_3$ ceramic with low dielectric loss. *J Am Ceram Soc* 1983;**66**:421–3.
8. Nomura S, Toyama K, Tanaka K. $Ba(Mg_{1/3}Ta_{2/3})O_3$ ceramics with temperature-stable high dielectric constant and low microwave loss. *Jpn J Appl Phys* 1982;**21**:L624–626.
9. Surendran KP, Sebastian MT, Mohanan P, Philip MV. The effect of dopants on the microwave dielectric properties of $Ba(Mg_{0.33}Ta_{0.67})O_3$ ceramics. *J Appl Phys* 2005;**98**:094114.
10. O'Bryan HMJ, Thomson JJ, Plourde JK. A new $BaO–TiO_2$ compound with temperature-stable high permittivity and low microwave loss. *J Am Ceram Soc* 1974;**57**:450–3.
11. Plourde JK, Linn DF, O'Bryan HMJ, Thompson JJ. $Ba_2Ti_9O_{20}$ as a microwave dielectric resonator. *J Am Ceram Soc* 1975;**58**:418–20.
12. Tamura H. Microwave loss quality of $(Zr_{0.8}Sn_{0.2})TiO_4$. *Am Ceram Soc Bull* 1994;**73**:92–5.
13. Wakino K. Miniaturization techniques of microwave components for mobile communications systems—using low loss dielectrics. *Ferroelectr Rev* 2000;**22**:1–49.
14. Fiedziuszko SJ, Hunter IC, Itoh T, Kobayashi Y, Nishikawa T, Stitzer SN, et al. Dielectric materials, devices, and circuits. *IEEE Trans Microwave Theory Tech* 2002;**50**:706–20.
15. Hernandez VS, Martinez LMT, Mather GC, West AR. Stoichiometry, structures and polymorphism of spinel-like phases, $Li_{1.33x}Zn_{2-2x}Ti_{1+067x}O_4$. *J Mater Chem* 1996;**6**:1533–6.
16. Kawai H, Tabuchi M, Nagata M, Tukamoto H, West AR. Crystal chemistry and physical properties of complex lithium spinels Li_2MM 'O-3(8) (M = Mg, Co, Ni, Zn; M' = Ti, Ge). *J Mater Chem* 1998;**8**:1273–80.
17. Hakki BW, Coleman PD. A dielectric resonator method of measuring inductive capacitance in the millimeter range. *IRE Trans Microwave Theory Tech* 1960;**MTT-8**:402–10.
18. Krupka J, Derzakowski KD, Riddle B, Jarvis JB. A dielectric resonator for measurements of complex permittivity of low loss dielectric materials as a function of temperature. *Meas Sci Technol* 1998;**9**:1751–6.
19. George S, Sebastian MT. Effect of lithium-based glass addition on the microwave dielectric properties of $Ca[(Li_{1/3}Nb_{2/3})_{1-x}T_{i-x}]_{3-\delta}$ ceramics for LTCC applications. *J Alloys Compd* 2009;**473**:336–40.
20. George S, Anjana PS, Deepu V, Mohanan P, Sebastian MT. Low-temperature sintering and microwave dielectric properties of Li_2MgSiO_4 ceramics. *J Am Ceram Soc* 2009;**92**:1244–9.
21. Cullity BD. *Elements of X-ray diffraction*. New Delhi: Printice Hall; 2001.
22. Penn SJ, Alford NM, Templeton A, Wang XR, Xu MS, Reece M, et al. Effect of porosity and grain size on the microwave dielectric properties of sintered alumina. *J Am Ceram Soc* 1997;**80**:1885–8.
23. Braginsky VB, Ilchenko VS, Bagdassarov KS. Experimental-observation of fundamental microwave-absorption in high-quality dielectric crystals. *Phys Lett A* 1987;**120**:300–5.
24. Gurevich VL, Tagantsev AK. Intrinsic dielectric loss in crystals. *Adv Phys* 1991;**40**:719–67.
25. Breeze JD, Perkins JM, McComb DW, Alford NM. Do grain boundaries affect microwave dielectric loss in oxides? *J Am Ceram Soc* 2009;**92**:671–4.
26. Alford NM, Penn SJ. Sintered alumina with low dielectric loss. *J Appl Phys* 1996;**80**:5895–8.
27. Roy R. Multiple ion substitution in perovskite lattice. *J Am Ceram Soc* 1954;**27**:581–8.
28. Li L, Chen XM, Fan XC. Characterization of $MgTiO_3–CaTiO_3$-layered microwave dielectric resonators with $TE_{01\delta}$ mode. *J Am Ceram Soc* 2006;**89**:557–61.
29. Liu T, Zhao XZ, Chen W. A/B site modified $CaTiO_3$ dielectric ceramics for microwave application. *J Am Ceram Soc* 2006;**89**:1153–5.
30. Jancar B, Valant M, Suvorov D. Solid-state reactions occurring during the synthesis of $CaTiO_3–NdAlO_3$ perovskite solid solutions. *Chem Mater* 2004;**16**:1075–82.
31. Moon JH, Jung HM, Park HS, Shin JY, Kim HS. Sintering behaviour and microwave dielectric properties of $(Ca,La)(Ti,Al)O_3$ ceramics. *Jpn J Appl Phys* 1999;**38**:6821–7.